Insular woody daisies (Argyranthemum, Asteraceae) are more resistant to drought-induced hydraulic failure than their herbaceous relatives

Larissa Dória, Diego Podadera, Marcelino del Arco, Thibaud Chauvin, Erik Smets, Sylvain Delzon, Frederic Lens

Received: 22 June 2017 | Accepted: 14 February 2018

DOI: 10.1111/1365-2435.13085

RESEARCH ARTICLE

Functional Ecology | BRITISH ECOLOGICAL SOCIETY

Insular woody daisies (*Argyranthemum*, Asteraceae) are more resistant to drought-induced hydraulic failure than their herbaceous relatives

Larissa C. Dória[1] | Diego S. Podadera[2] | Marcelino del Arco[3] | Thibaud Chauvin[4,5] | Erik Smets[1] | Sylvain Delzon[6] | Frederic Lens[1]

[1]Naturalis Biodiversity Center, Leiden University, Leiden, The Netherlands; [2]Programa de Pós-Graduação em Ecologia, UNICAMP, Campinas, São Paulo, Brazil; [3]Department of Plant Biology (Botany), La Laguna University, La Laguna, Tenerife, Spain; [4]PIAF, INRA, University of Clermont Auvergne, Clermont-Ferrand, France; [5]AGPF, INRA Orléans, Olivet Cedex, France and [6]BIOGECO INRA, University of Bordeaux, Cestas, France

Correspondence
Frederic Lens
Email: frederic.lens@naturalis.nl

Funding information
Conselho Nacional de Desenvolvimento Científico e Tecnológico, Grant/Award Number: 206433/2014-0; French National Agency for Research, Grant/Award Number: ANR-10-EQPX-16 and ANR-10-LABX-45; Alberta Mennega Stichting

Handling Editor: Rafael Oliveira

Abstract

1. Insular woodiness refers to the evolutionary transition from herbaceousness towards derived woodiness on (sub)tropical islands and leads to island floras that have a higher proportion of woody species compared to floras of nearby continents.
2. Several hypotheses have tried to explain insular woodiness since Darwin's original observations, but experimental evidence why plants became woody on islands is scarce at best.
3. Here, we combine experimental measurements of hydraulic failure in stems (as a proxy for drought stress resistance) with stem anatomical observations in the daisy lineage (Asteraceae), including insular woody *Argyranthemum* species from the Canary Islands and their herbaceous continental relatives.
4. Our results show that stems of insular woody daisies are more resistant to drought-induced hydraulic failure than the stems of their herbaceous counterparts. The anatomical character that best predicts variation in embolism resistance is intervessel pit membrane thickness (T_{PM}), which can be functionally linked with air bubble dynamics throughout the 3D vessel network. There is also a strong link between T_{PM} vs. degree of woodiness and thickness of the xylem fibre wall vs. embolism resistance, resulting in an indirect link between lignification and resistance to embolism formation.
5. Thicker intervessel pit membranes in *Argyranthemum* functionally explain why this insular woody genus is more embolism resistant to drought-induced failure compared to the herbaceous relatives from which it has evolved, but additional data are needed to confirm that palaeoclimatic drought conditions have triggered wood formation in this daisy lineage.

KEYWORDS

Canary Islands, drought, hydraulic failure, insular woodiness, lignification, stem anatomy, thickness of intervessel pit membrane, xylem hydraulics

1 | INTRODUCTION

It has been known for a long time that island floras have a higher proportion of woody species compared to adjacent continents, and related species on islands are often woodier than their continental relatives (Carlquist, 1974; Darwin, 1859; Wallace, 1878). This phenomenon refers to insular woodiness and describes the evolutionary transition from herbaceous towards (derived) woody flowering plant species on (sub)tropical oceanic islands (e.g. Carlquist, 1974; Lens, Davin, Smets, & del Arco, 2013). Interestingly, woodiness is considered to be ancestral within flowering plants (Doyle, 2012), meaning that herbaceous lineages lost woodiness that characterized their ancestrally woody ancestors. This implies that the transition from herbaceousness towards insular woodiness (only on islands) or derived woodiness (on islands and continents) represents an evolutionary reversal back to the woody state (Lens, Davin et al., 2013). A number of hypotheses have been put forward to explain insular woodiness, such as (1) increased competition hypothesis (taxon-cycling hypothesis; Darwin, 1859; Givnish, 1998), (2) greater longevity hypothesis (promotion-of-outcrossing hypothesis; Böhle, Hilger, & Martin, 1996; Wallace, 1878), (3) moderate climate hypothesis (Carlquist, 1974) and (4) reduced herbivore hypothesis (Carlquist, 1974). However, experimental data for these hypotheses are non-existing or based on only a few, small-scale examples. A recent review on insular woodiness of the Canary Islands showed that a majority of the insular woody species grow in dry coastal regions (Lens, Davin et al., 2013), and an ongoing global derived woodiness database at the flowering plant level reveals a strong drought signal (F. Lens, unpublished data), suggesting a functional link between wood formation and increased drought stress resistance. Experimental support for this link was found in *Arabidopsis thaliana* (Lens, Smets, & Melzer, 2012) using xylem physiological measurements in stems, but not a single study has compared drought-induced hydraulic failure with stem anatomy between derived woody plants and their herbaceous relatives growing in nature.

Hydraulic failure has been put forward as one of the prime mechanisms underlying drought-induced mortality in plants (Adams et al., 2017; Anderegg et al., 2016) and corresponds to the disruption of water transport in embolized xylem conduits when plants face drought (Lens, Tixier et al., 2013). As the proportion of gas embolism in xylem conduits generally enhances with increasing drought stress, the hydraulic conductivity decreases until a critical threshold, potentially leading to plant death (Adams et al., 2017; Brodribb, Bowman, Nichols, Delzon, & Burlett, 2010; Urli et al., 2013). Plant resistance to embolism is estimated using so-called vulnerability curves, from which the P_{50}, that is the xylem pressure inducing 50% loss of hydraulic conductivity, can be estimated (Cochard et al., 2013). P_{50} measurements have been carried out for hundreds of (ancestrally) woody species (Bouche et al., 2014; Choat et al., 2012; Maherali, Pockman, & Jackson, 2004) and show that the species from dry environments are generally more resistant to embolism (more negative P_{50}) than species from wet climates (Choat et al., 2012; Larter et al., 2015; Lens, Tixier et al., 2013; Lens et al., 2016). In contrast, vulnerability curves from herbaceous and derived woody stems remain limited to only a few dozen species (Lens et al., 2016).

In this study, we want to assess for the first time the correlation between embolism resistance and insular woodiness by complementing hydraulic stem observations with detailed light microscope and electron microscope observations in the insular woody *Argyranthemum* and its close continental relatives (tribe Anthemideae, family Asteraceae). More specifically, we will address whether this correlation would be functional or rather indirect due to the presence of a vessel feature that is functionally linked with both embolism resistance and increased woodiness in this daisy clade. The woody genus *Argyranthemum*, deeply nested into the predominantly herbaceous lineage including subtribes Leucantheminae, Santolininae and Glebionidinae, is the largest plant genus endemic to the volcanic Macaronesian archipelago and has the Mediterranean herbaceous *Glebionis* and *Ismelia* (Glebionidinae) as closest relatives (Oberprieler et al., 2009). *Argyranthemum* encompasses 24 species endemic to the islands of Madeira, Selvagens and the Canaries (Humphries, 1976) and predominantly inhabits the dry coastal desert and more humid lowland scrub vegetation, although some species have also invaded the other major habitats of the Canary archipelago (Francisco-Ortega, Crawford, Santos-Guerra, & Jansen, 1997).

The main objectives in our study are (1) to investigate whether the insular woody stems of *Argyranthemum* are more resistant to drought-induced hydraulic failure than those of their herbaceous relatives, (2) to find (non-)functional stem anatomical characters that best explain the observed variation in P_{50} between the daisy species observed and (3) to assess whether the woody species native to drier habitats are more resistant to embolism formation compared to *Argyranthemum* species growing in wetter habitats.

2 | MATERIALS AND METHODS

2.1 | Plant material

During different field campaigns (May 2013, January 2014 and November 2015; Figure S1), we collected species of the perennial woody *Argyranthemum* (subtribe Glebionidinae) throughout the island of Tenerife, situated near the centre of the Canary Island archipelago in the Atlantic Ocean off the coast of north-western Africa (Del-Arco et al., 2006).

We selected the rainy period of Tenerife (November–March) to collect our specimens to avoid high native levels of drought-induced embolism in the stems. For each of the woody individuals studied, we collected at least two 50-cm-long stem samples, from the main stem and/or from the proximal branches (depending on the size of the individual), from 10 individuals per species: *A. adauctum*, *A. broussonetii*, *A. foeniculaceum*, *A. frutescens* and *A. gracile* (Figure S1). All the woody species collected are deciduous, except for the evergreen *A. broussonetii* and *A. adauctum* collected at the laurel forest and humid high-altitude zones on Tenerife, respectively.

For comparison with the closely related herbaceous species, we collected *Leucanthemum vulgare* (Leucantheminae subtribe),

the only perennial herbaceous species, on the campus of Bordeaux University (France), and performed the measurements during May–June 2013. The other closely related herbaceous species, *Glebionis coronaria*, *G. segetum* (belonging to subtribe Glebionidinae), *Cladanthus mixtus* (Santolininae subtribe) and *Coleostephus myconis* (Leucantheminae subtribe), are all annuals and were collected on the island of Tenerife, Canary Islands (Figure S1), during their flowering period (March 2016). All the herbaceous species collected on Tenerife are continental species that have invaded the Canaries recently (Arechavaleta, Rodriguez, Zurita, & García, 2010). Between 10 and 20 individuals of each herbaceous species were harvested.

In the field, we collected straight woody branches of at least 35 or 50 cm long for the standard (27 cm diameter) and medium Cavitron (42 cm diameter), respectively. The branches were cut in air, immediately wrapped in wet tissues and sealed in a dark plastic bag. For the herbaceous species, entire individuals were collected, with roots still attached. Afterwards, stems were stored in a cold room (around 5°C) for a few days in the University of La Laguna, Tenerife, before being shipped by plane to the high-throughput caviplace platform (University of Bordeaux, France).

2.2 | Xylem vulnerability to embolism

Prior to measurement, all the branches were cut under water in the laboratory with a razor blade into a standard length of 27 or 42 cm to fit the two Cavitron rotors (Cochard, 2002; Cochard et al., 2013); bark was removed for the woody species. The stems were not flushed prior to the measurements to avoid cavitation fatigue as a result of potential damage of intervessel pit membranes (Hacke, Stiller, Sperry, Pittermann, & McCulloh, 2001). First, the maximum conductivity of the stem in its native state (K_{max} in $m^2\ MPa^{-1}\ s^{-1}$) was calculated under xylem pressure close to zero MPa using a reference ionic solution of 10 mM KCl and 1 mM $CaCl_2$ in deionized ultrapure water. Then, rotation speed of the centrifuge was gradually increased by −0.5 or −1 MPa, to lower xylem pressure. The percentage loss of conductivity (PLC) of the stem was determined at each pressure step following the equation:

$$PLC = 100 \times \left(1 - \frac{K}{K_{max}}\right) \quad (1)$$

where K_{max} represents the maximum conductance of the stem at the lowest pressure applied (−0.5 MPa) and K represents the conductance associated at each pressure step.

The vulnerability curves, showing the relation between the xylem pressure and the percentage loss of conductivity, were obtained using the Cavisoft software (Cavisoft v1.5, University of Bordeaux, Bordeaux, France). A sigmoid function (Pammenter & Van der Willigen, 1998) was fitted to the data from each sample, using the next equation with SAS 9.4 (SAS 9.4; SAS Institute, Cary, NC, USA):

$$PLC = \frac{100}{\left[1 + \exp\left(\frac{s}{25} \times (P - P_{50})\right)\right]} \quad (2)$$

where S (% per MPa^{-1}) is the slope of the vulnerability curve at the inflexion point, P is the xylem pressure value used at each step and P_{50} is the xylem pressure inducing 50% loss of hydraulic conductivity. The parameters S and P_{50} were averaged for each species (n = 10).

2.3 | Wood anatomy

Light microscopy (LM), scanning electron microscopy (SEM) and transmission electron microscopy (TEM) observations were performed at Naturalis Biodiversity Center based on the samples for which we have obtained suitable vulnerability curves. The samples were taken from at least two individuals per species, from the middle part of the stem segment where the negative pressure caused embolism formation during the Cavitron experiment, which reflects the in vivo conditions of a plant experiencing drought stress. All the anatomical measurements (Table 1) were taken using ImageJ (National Institutes of Health, Bethesda, USA), following largely the suggestions of Scholz, Klepsch, Karimi, and Jansen (2013) and IAWA Committee (1989).

For LM, the woody species were cut in transverse and tangential sections of 20 μm thickness using a sliding microtome (Reichert, Vienna, Austria). After bleaching with sodium hypochlorite 1%–3% and rinsing with water, the sections were briefly stained with a 1:2 mixture of safranin (0.5% in 50% ethanol) and alcian blue (1% in water), dehydrated in an ethanol series (50%, 70%, 96%), treated with a Parasolve clearing agent (Prosan, Merelbeke, Belgium) and mounted in Euparal (Waldeck GmbH & Co. KG, Germany; Lens et al., 2011). For the herbaceous species, the samples were embedded in LR-White resin following Hamann, Smets, and Lens (2011). Transverse sections of 4 μm were made using a rotary microtome (Leica RM 2265), heat fixed to the slide, stained with toluidine blue (0.1% in water) and mounted in Entellan®. The sections were observed using a Leica DM2500 light microscope and photographed with a Leica DFC-425C digital camera (Leica microscopes, Wetzlar, Germany). The diameter of vessels (D_V) was calculated based on the lumen area that was considered to be a circle following the equation:

$$D_V = \sqrt{\frac{4A}{\pi}} \quad (3)$$

where D_V is the vessel diameter and A is the vessel lumen area. The hydraulically weighted vessel diameter (D_{HV}) was calculated following the equation (Sperry, Nichols, & Sullivan, 1994):

$$D_{HV} = \frac{\sum D_V^5}{\sum D_V^4} \quad (4)$$

where D_V is the vessel diameter as measured in Equation 3. We also calculated D_{HV} according to the Tyree and Zimmermann (2002) equation: $D_{HV} = \left(\sum D_V^4 / n\right)^{1/4}$, where n is the number of vessels measured (Table S3), but used Equation 4 in our statistics analyses as there is no consensus at this point preferring one calculation over

TABLE 1 List with the anatomical characters measured, their symbols and units, and the type of microscopy applied

Acronym	Definition	Calculation	Units	Technique
D_V	Diameter of vessels	Equation 3	μm	LM
D_{HV}	Hydraulically weighted vessel diameter	Equation 4	μm	LM
DE_V	Density of vessels	Number of vessel counted in random selection of five zones of 1-mm^2 wood area	No. of vessels/mm^2	LM
G_V	Vessel grouping index	Total number of vessels divided by the total number of vessel groupings (incl. solitary and grouped vessels)	No. of vessels/vessel group	LM
T_W:D_V	Thickness-to-span ratio of vessels	Double intervessel wall thickness divided by maximum vessel diameter in vessel group	-	LM
A_S	Total stem area	Total stem area in cross section	μm^2	LM
A_{LIG}	Lignified stem area	Total xylem area + fibre caps area in cross section	μm^2	LM
A_{PITH}	Pith area	Total pith area in cross section	μm^2	LM
A_F	Xylem fibre cell area	Area of single xylem fibre in cross section	μm^2	LM
A_{FL}	Xylem fibre lumen area	Area of single xylem fibre lumen in cross section	μm^2	LM
A_{FW}	Xylem fibre wall area	A_F minus A_{FL} for the same fibre	μm^2	LM
P_{LIG}	Proportion of lignified area per total stem area	A_{LIG}: A_S	–	LM
P_{PITH}	Proportion of pith per total stem area	A_{PITH}: A_S	–	LM
$P_{FW}F$	Proportion of xylem fibre wall per fibre	A_{FW}: A_F for the same fibre; measure of xylem fibre wall thickness	–	LM
H_R	Height of rays	Measured in tangential section only for woody species	μm	LM
DE_R	Density of rays	Total number of rays per mm^2 as measured in tangential section (only for woody species)	N° of rays/mm^2	LM
P_R	Proportion of ray area per wood area	Total area of rays per mm^2 of tangential section (only for woody species)	–	LM
A_{PB}	Intervessel pit border area	Area of single intervessel pit border in tangential surface	μm^2	SEM
A_{PA}	Intervessel pit aperture area	Area of single intervessel pit aperture in tangential surface	μm^2	SEM
F_{PA}	Intervessel pit aperture fraction	A_{PA}: A_{PB} for the same pit	–	SEM
T_{PM}	Thickness of intervessel pit membrane	Thickness of intervessel pit membrane near the centre of a relaxed (non-aspirated) membrane	nm	TEM
D_{PC}	Depth of intervessel pit chamber	Distance from the pit membrane to the inner pit aperture	nm	TEM

the other, and because there is a linear relationship between the D_{HV} values derived from both equations.

For SEM, dried wood specimens from two individuals per species were split in a tangential plane, dehydrated in an ethanol series (50%, 70%, 96%), dried at room temperature, fixed to aluminium stubs with an electron-conductive carbon sticker, platinum-/palladium-coated with a sputter coater (Quorum Q150TS Quorum Technologies, Laughton, UK) and observed with a field emission SEM (Jeol JSM-7600F, Tokyo, Japan) at a voltage of 5 kV to observe the intervessel pits.

For TEM, fresh pieces from the outer part of the xylem were cut into 2-mm^3 blocks and immediately fixed 48 hr in Karnovsky's fixative (Karnovsky, 1965). Subsequently, the samples were rinsed in 0.1 M cacodylate buffer, post-fixed with 1% buffered osmium tetroxide for 3 hr at room temperature and rinsed again with buffer solution. Subsequently, the samples were stained with 1% uranyl acetate, dehydrated through a graded propanol series (30%, 50%, 70%, 96% and 100%) and acetonitrile and embedded in Epon 812 n (Electron Microscopy Sciences, Hatfield, England) at 60°C for 48 hr. After embedding, 2-μm-thick cross sections were cut from the resin blocks with a glass knife to observe areas including adjacent vessels. The cross-sectional areas from the resin blocks were then trimmed to maintain only vessel–vessel contact areas, and 90-nm-thick cross sections were made with a diamond knife. The sections were dried on 300-mesh copper grids with Formvar coating (Agar Scientific, Stansted, UK). Several grids were prepared for each resin sample and manually counterstained with uranyl acetate and lead citrate.

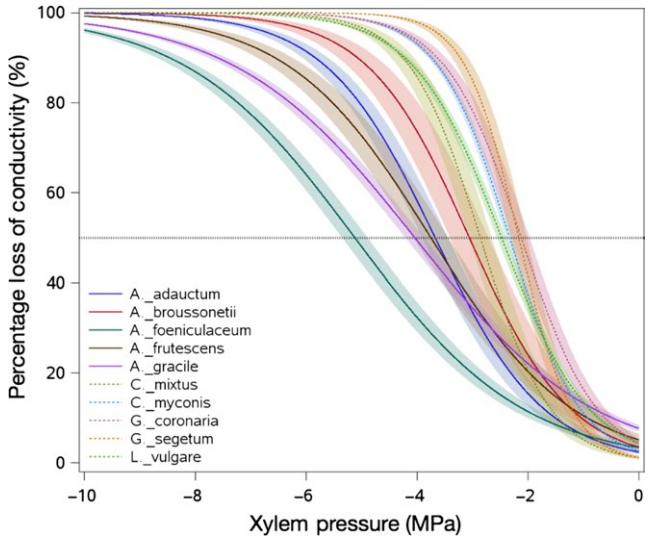

FIGURE 1 Mean vulnerability curve for each of the 10 species studied showing percentage loss of conductivity (%) as a function of xylem pressure (MPa). The plain curves indicate the VCs for the woody species, and the dotted VCs represent the herbaceous species. Shaded bands represent standard errors

Ultrastructural observations were carried out on intervessel pits with relaxed (non-aspirated) membranes using a JEOL JEM 1400-Plus TEM (JEOL, Tokyo, Japan), equipped with a 11 MPixel camera (Quemesa, Olympus) based on at least 20 observations per individual. As we only observed intervessel pit membranes from the central stem segment parts where centrifugal force was applied, our measurements provide a relative estimation of intervessel pit membrane thickness.

2.4 | Statistics

To test the difference between P_{50}, P_{12} (pressure inducing 12% loss of hydraulic conductivity referring to initial air-entry pressure), P_{88} (pressure inducing 88% loss of hydraulic conductivity referring to irreversible death-inducing xylem pressure in angiosperms; Barigah et al., 2013; Urli et al., 2013) and S (slope of vulnerability curve at inflexion point, an indicator for the speed at which embolisms affect the stem) with life form (woodiness vs. herbaceousness), we used generalized least squares (GLS). To deal with heteroscedasticity, we included a varIdent weights function (Zuur, Ieno, Walker, Saveliev, & Smith, 2009). Statistical analyses were carried out using the gls function from the nlme package (Pinheiro, Bates, DebRoy, & Sarkar, 2016) in the R software (R Core Team 2016).

To test which stem anatomical characters best explain embolism resistance, we performed a multiple linear regression, with the P_{50} as response variable and the stem anatomical characters as predictive variables. As several of the anatomical features measured were correlated, we selected a priori the predictive variables using the following criteria: biological insights based on previously published studies and a pairwise scatterplot to detect relationship between response variable and predictive variables. To assess high multicollinearity amongst predictive variables, we conducted a variance inflation factor (VIF) analysis, keeping only variables with a VIF value lower than two (Zuur, Ieno, & Elphick, 2010). Subsequently, we performed the stepwise function using the direction method "both" of the "step" function from "stats" package (R Core Team 2016). The regression or differences was considered to be significant if $p \leq .05$. Further, we calculated the hierarchical partitioning (Chevan & Sutherland, 1991) for the significant variables retained in the model in order to assess their relative importance to explain the P_{50}.

We performed simple linear regression between thickness of intervessel pit membrane (T_{PM}) and P_{50} to assess a potential correlation. To deal with heteroscedasticity, we included a varFixed weights function (Zuur et al., 2009). We calculate the R^2 values based on the method of Nakagawa and Schielzeth (2013), using the function rsquared in the package piecewiseSEM (Lefcheck, 2015). Furthermore, the regression was applied between P_{50} and the proportion of lignified area per total stem area (P_{LIG}) for eight individuals measured of *Cladanthus mixtus* due to the high intraspecific variation in the degree of woodiness for this species.

To assess the correlation between the predictive variables and P_{50} in the general dataset (woody + herbaceous species studied), as well as in the woody and herbaceous dataset separately, we performed Pearson's or Spearman's correlation analyses depending on the normality of the variable's distribution. P_{LIG} in the general dataset was log-transformed to match the normality. Finally, we performed a Student's *t* test to assess the difference in pit membrane thickness between the insular woody and herbaceous group.

3 | RESULTS

3.1 | Xylem vulnerability to embolism in the daisy group

The insular woody daisy species are more embolism resistant than their herbaceous relatives (Figures 1 and 2a–d; Table S1). The vulnerability curves used to construct the average curve were all S-shaped (Figure S2). P_{50} varied twofold across species, with significant variation in P_{50} between woody and herbaceous species ($F = 66.45$; $p < .0001$). Similar significant variation in P_{88} ($F = 90.03$; $p < .0001$) was also observed, but not for P_{12} ($F = 1.61$; $p = .20$). The P_{50} ranged from −2.1 MPa for the herbaceous *Glebionis coronaria* up to −5.1 MPa for the woody *A. foeniculaceum* (Figure 1; Table S1). Amongst the woody species, the most vulnerable species is *A. broussonetii* ($P_{50} = -3.1$ MPa), while *Cladanthus mixtus* is the herbaceous species most resistant to embolism ($P_{50} = -2.9$ MPa; Figure 1; Table S1). Amongst the herbaceous species, *C. mixtus* shows the largest variation in P_{50}, ranging from −1.9 MPa till −4.1 MPa (Figure 1), but intraspecific variation for most other herbaceous species measured is limited.

The vulnerability curve slopes are significantly higher for the herbaceous species ($F = 67.77$; $p < .0001$). Slopes of the vulnerability curves varied threefold across species, with the lowest slope of 16% MPa^{-1} for the woody *A. foeniculaceum* and the steepest slope of 52% MPa^{-1} for the herbaceous *Glebionis segetum* (Table S1).

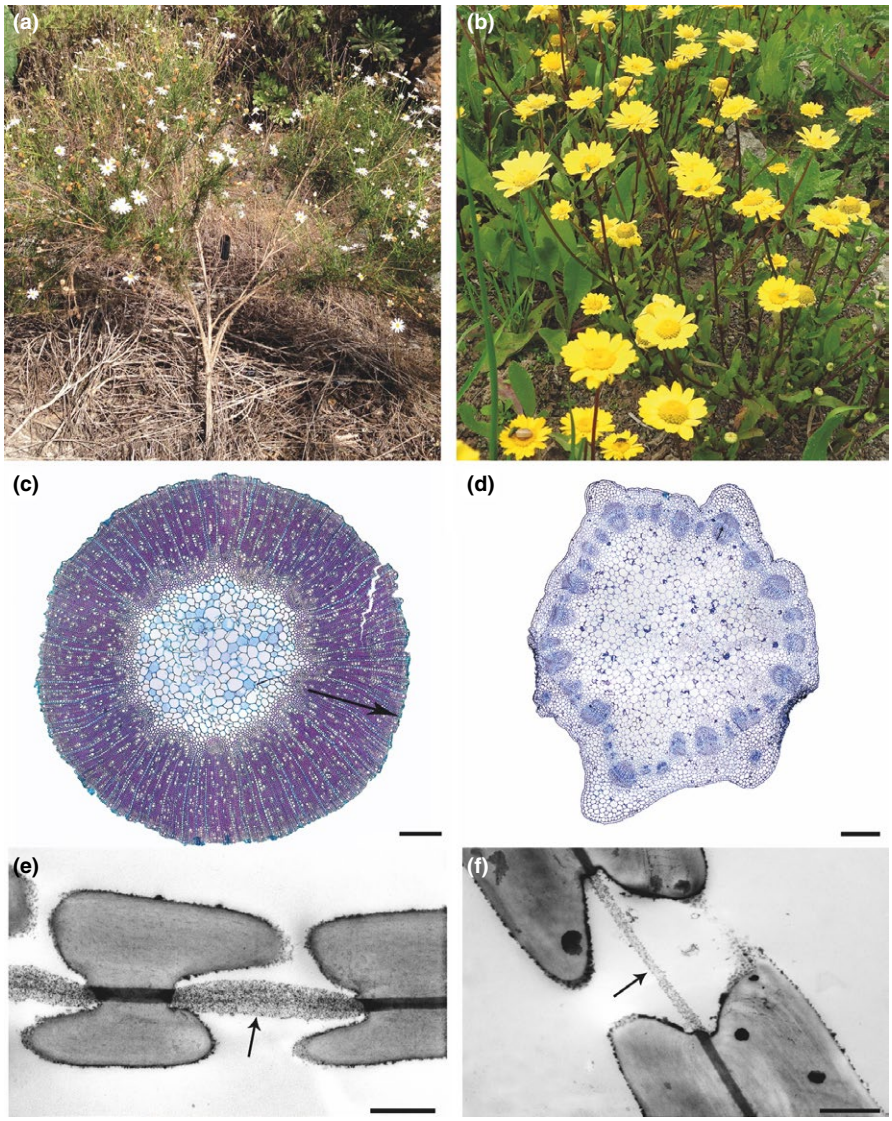

FIGURE 2 Illustration of life form and hydraulically relevant anatomical features of *Argyranthemum gracile* (left) and *Coleostephus myconis* relative (right). (a, b) species in the field; (c, d) light microscope images of stem cross sections, the arrows show the marked difference in xylem area; (e, f) transmission electron microscopy (TEM) images of intervessel pit membranes (arrows) showing thicker membranes in the woody *A. gracile* (e) compared to the herbaceous *C. myconis* (f). Scale bars represent 500 μm (c, d), 1 μm (e, f)

TABLE 2 Multiple regression model of anatomical features explaining the variance in the P_{50} in woody and herbaceous daisies. The values in bold indicate significant correlation ($p < .05$)

Source of variation	Parameter estimate	*SE*	*t*-value	*p*-Value	Hierarchical partitioning	VIF values
T_{PM}	−0.0096	0.0020	−4.890	**.0027**	70.30%	1.2560
$P_{FW}F$	−4.5862	1.8420	−2.490	**.0471**	29.70%	1.2453
D_{HV}	−0.0591	0.0285	−2.072	.0836		1.0169

T_{PM}, thickness of intervessel pit membrane; $P_{FW}F$, proportion of xylem fibre wall per fibre; D_{HV}, hydraulically weighted vessel diameter.

3.2 | Relationship between embolism resistance and wood anatomy

A combined backward and forward multiple regression analysis shows that the thickness of intervessel pit membrane (T_{PM}), the proportion of xylem fibre wall per fibre ($P_{FW}F$) and the hydraulically weighted diameter of vessels (D_{HV}) best explain the variation in P_{50} ($p = .0018$, $R^2 = .8578$; Table 2). However, only T_{PM} and $P_{FW}F$ are significant, with T_{PM} explaining 70% and $P_{FW}F$ 30% of the variation in P_{50} (Table 2).

In the general dataset, the thickness of intervessel pit membrane (T_{PM}) correlates with embolism resistance ($p = .0021$, $R^2 = .4425$; Figure 3a): the more resistant insular woody species (proportion of lignified area per total stem area ranging from 0.70 to 0.84) show thicker intervessel pit membranes than the vulnerable herbaceous species (proportion of lignified area per total stem area ranging from

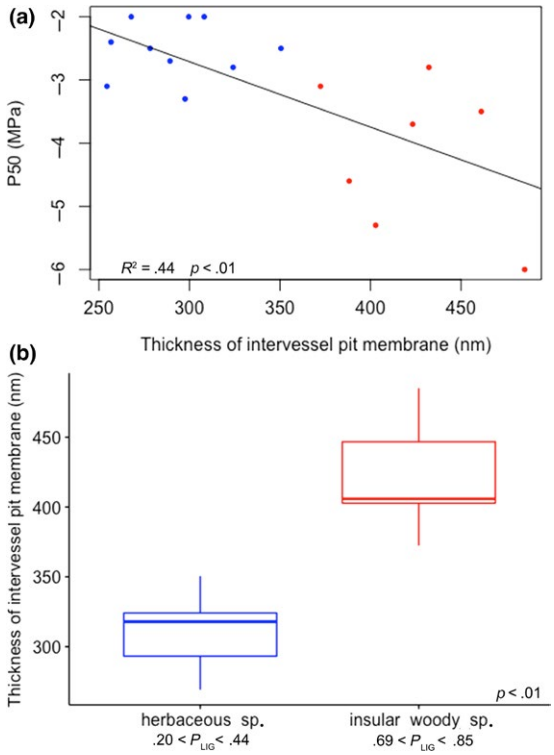

FIGURE 3 Thickness of intervessel pit membrane (T_{PM}) and its significant relationship to embolism resistance (a), life form—lignification (b). P_{LIG} = proportion of lignified area per total stem area. Red refers to insular woody species and blue to herbaceous species. Each dot relates to one individual. The bottom, middle and upper lines of the box represent the 25th quartile, the median and the 75th quartile, respectively. Upper and bottom ends of the vertical lines indicate the maximum and minimum values of T_{PM}

0.21 to 0.43; *t* test, p = .0017; Figures 2e,f and 3b). T_{PM} is also correlated with vessel grouping index in the general dataset and in the woody dataset (p = .0448, r = .6440; p = .0221, r = .9297), respectively. Aspirated intervessel pit membranes were very scarce and ignored in our measurements.

In addition to the thickness of intervessel pit membrane (Figure 3a), the following anatomical variables in the general dataset (herbaceous and woody species combined; Table S2) are significantly correlated with P_{50}: density of vessels (p = .0028; r = −.8317), vessel grouping index (p = .0040; r = −.8151) and the proportion of lignified area per total stem area (p = .0060; r = −.7952; Figure 2c,d). However, when we analyse the woody species separately (Table S2), only vessel grouping index (p = .0055; r = −.9722) and proportion of ray area per wood area (p = .04997; r = −.8784) are significantly correlated with P_{50}, whereas all the significant correlations disappear in the herbaceous dataset probably due to the limited variation in P_{50} amongst the herbaceous species studied (Tables S1 and S2). The axial parenchyma patterns are very similar between the most resistant and most vulnerable *Argyranthemum* species (scanty paratracheal according to IAWA Committee, 1989).

The simple linear regression for *C. mixtus* individuals shows that the proportion of lignified area per total stem area is highly linked with P_{50} for this population (p = .0008; R^2 = .84; Figure 4e), which scales with the large intraspecific variation in the degree of woodiness in the stem (Figure 4a–d).

4 | DISCUSSION

4.1 | Stems of insular woody daisies are more embolism resistant than those of their herbaceous relatives

Our xylem physiological embolism resistance data show one major outcome: stems of the insular woody *Argyranthemum* are more resistant to drought-induced hydraulic failure than those of their herbaceous Anthemideae relatives. Additionally, the difference in slopes of the vulnerability curves between woody and herbaceous species demonstrates that embolism formation occurs slower in the former (Figure 1; Table S1). The positive link between increased wood formation and embolism resistance within the daisy lineage matches the observation that insular woody species native to the Canary Islands are often distributed in the dry coastal areas (Lens, Davin et al., 2013) and agrees with an ongoing global derived woodiness database at the flowering plant level, comprising more than 6,000 species of which most of them are native to regions with a marked drought period such as (semi-)deserts, savannas, steppes and Mediterranean-type habitats (F. Lens, unpublished data). Despite the overwhelming evidence for this positive link, it is hard to functionally explain why derived woody species are better adapted to drought compared to their herbaceous relatives, as at first sight, there seems to be no evidence for a direct functional link between increased wood formation and increased drought stress resistance. Obviously, woody species have more reinforced conduit and fibre walls, which indirectly relates to embolism resistance and directly relates to conduit implosion resistance (Hacke, Sperry, Pockman, Davis, & McCulloh, 2001; Jacobsen, Ewers, Pratt, Paddock, & Davis, 2005), although P_{50} values seem to be well above the implosion limit in angiosperm stem xylem (Sperry, 2003). Furthermore, there is a correlation between vessel wall thickness and intervessel pit membrane thickness (Jansen, Choat, & Pletsers, 2009; Li et al., 2016), meaning that vessel wall thickness is indirectly correlated with embolism resistance via air-seeding. Likewise, it is possible that reinforced vessel and neighbouring fibre walls better avoid microcracks through which embolism nucleation may occur or air could be sucked in (Jacobsen et al., 2005; see following two sections).

Second, P_{50} seems to behave as an important adaptive trait to survive drought stress within *Argyranthemum*, as the most vulnerable woody species—the evergreen *A. broussonetii*—was sampled in the wet laurel forests, while most other more resistant *Argyranthemum* species are native to drier habitats (Figure 1; Figure S1). Similar correlations between P_{50} and precipitation have been identified in many other lineages (Choat et al., 2012; Larter et al., 2015; Lens et al., 2016; Maherali et al., 2004; Trueba et al., 2017).

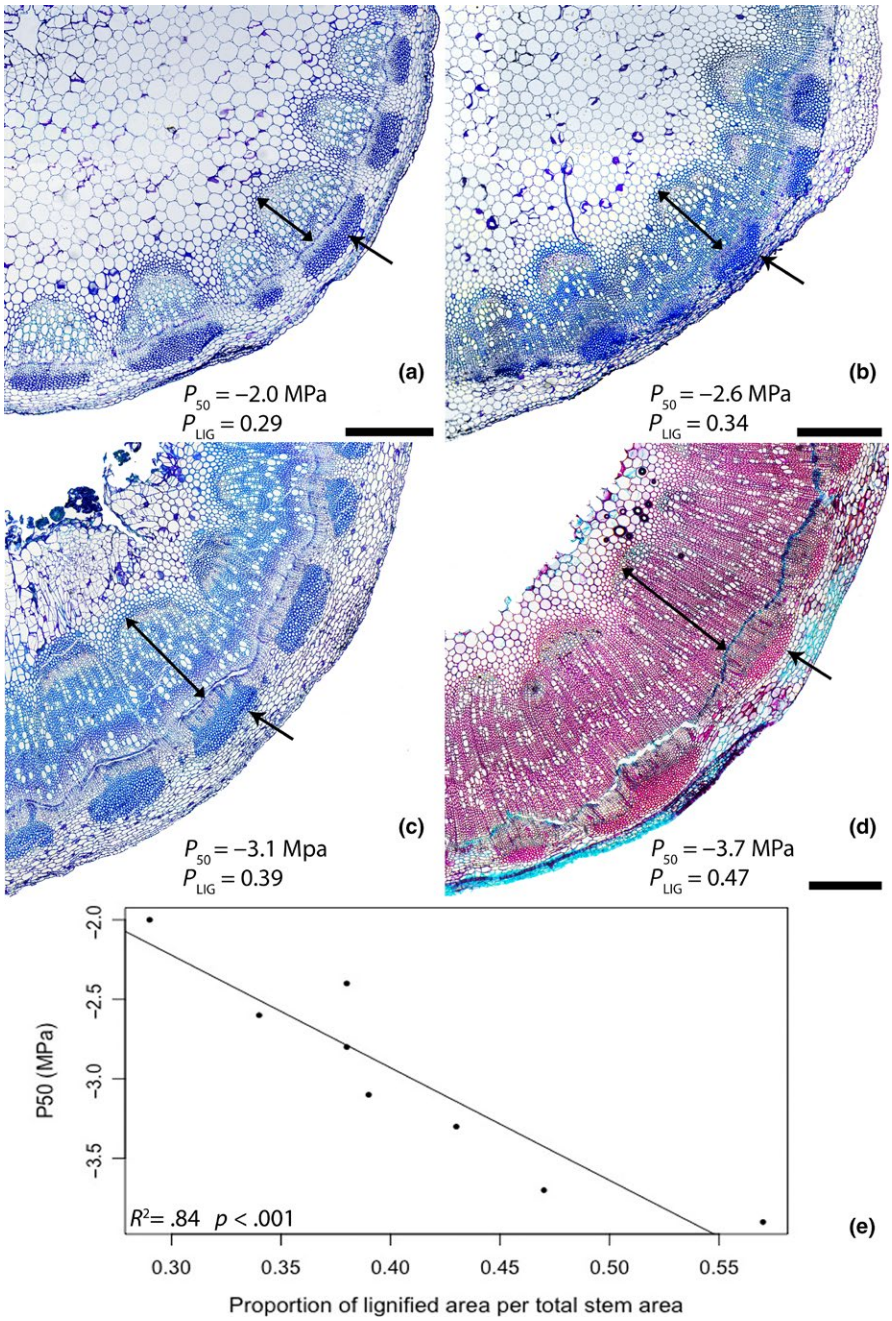

FIGURE 4 The intraspecific variation in the proportion of lignified area per total stem area (P_{LIG}) amongst *Cladanthus mixtus* individuals and its relation with P_{50}. (a–d) In ascending order, LM images of cross sections showing the P_{LIG}–P_{50} relationship. (e) Fitted linear model between P_{50} and P_{LIG}. Double arrow heads indicate the xylem area; single arrow heads point to extraxylary fibre caps. Each dot relates to one individual. Scale bars represent 500 μm

4.2 | Variation in intervessel pit membrane thickness (T_{PM}) is essential to explain differences in drought-induced hydraulic failure within the daisy lineage

The anatomical variable that could explain the abovementioned indirect link between insular woodiness and increased embolism resistance must be correlated with both increased wood formation, measured as a higher proportion of lignified area per total stem area (P_{LIG}), and with P_{50} and must also functionally explain embolism formation and/or spread within the 3D vessel network. Intervessel pit membrane thickness (T_{PM}) is the ideal candidate to clarify this indirect link, because it matches all criteria: (1) T_{PM} is tightly linked with life form (referring to the proportion of lignified area per total stem area; Figure 3b) as well as P_{50} (Figure 3a), (2) T_{PM} is the most significant variable in the regression model (explaining 70% of the P_{50} variation; Table 2), highlighting its hydraulic relevance as the best predictor of embolism resistance amongst the daisy species studied (Figure 2e,f; Table 2), and (3) the functional aspect of the observed T_{PM}–P_{50} correlation is obvious due to air-seeding, as more embolism-resistant daisies have thicker intervessel pit membranes (Figures 2e,f and 3b; Table S3). The thickness of intervessel pit membrane is likely to affect the length of the tortuous and irregularly shaped pores that air–water menisci need to cross before air-seeding may occur, explaining the spread of embolism through intervessel pit membranes into adjacent conduits, and thereby emphasizing its direct functional

link with respect to embolism resistance (Jansen et al., 2009; Lens, Tixier et al., 2013; Lens et al., 2011; Li et al., 2016). New findings reveal that the likelihood of bubble snap-off is higher when air passes the longer and more tortuous pore pathway of thicker intervessel pit membranes compared to thinner membranes. It is believed that the lipid-based surfactants molecules in the intervessel pit membrane pores ensure coating of these so-called nanobubbles, while they lower their dynamic, concentration-dependent surface tension and thereby stabilize the bubbles under negative pressure (Schenk, Steppe, & Jansen, 2015; Schenk et al., 2017).

4.3 | The relationship between increased embolism resistance and increased wood formation/lignification is strong but indirect

In addition to the observed correlation between the proportion of lignified area per total stem area (P_{LIG}) and embolism resistance (Table S2), we have also found another lignification link in our dataset: the proportion of xylem fibre wall per fibre ($P_{FW}F$), which is a measure for fibre wall thickness in the xylem, explains 30% of the variation in P_{50} (Table 2). As lignification in angiosperm shrubs and trees is mainly defined by wood fibres (Zieminska, Butler, Gleason, Wright, & Westoby, 2013; Zieminska, Westoby, & Wright, 2015), and as wood lignin content is positively linked to embolism resistance in a global dataset (Pereira, Domingues-Junior, Jansen, Choat, & Mazzafera, 2017), our observed (indirect) correlation between the proportion of xylem fibre wall per fibre and P_{50} could be expected. Likewise, further support for the strong positive link between lignification and embolism resistance is provided by other sources of data, such as wood density (Jacobsen et al., 2005; Hoffman, Marchin, Abit, & Lau, 2011; but see meta-analyses by Anderegg et al., 2016 and Gleason et al., 2016), conduit wall thickness (Cochard, Barigah, Kleinhentz, & Eshel, 2008; Hacke, Sperry et al., 2001; Jansen et al., 2009) and fibre wall area (Jacobsen et al., 2005). Moreover, the link between lignification and embolism resistance has been experimentally demonstrated in grasses (Lens et al., 2016), in the wild-type and woody mutant of *Arabidopsis thaliana* (Lens, Smets et al., 2012) and in several transgenic poplars modified for lignin metabolism (Awad et al., 2012). Based on these observations, it seems that many plant lineages invest much energy to develop a mechanically stronger, embolism-resistant stem (Lens, Tixier et al., 2013; Lens et al., 2016; Pereira et al., 2017).

Interestingly, the correlation between the degree of lignification and P_{50} is also confirmed within the herbaceous *Cladanthus mixtus*, where the more embolism-resistant individuals (P_{50} ranging from −3.1 MPa to −3.7 MPa) have more lignified stems compared to the more vulnerable individuals (P_{50} ranging from −1.2 MPa to −2.8 MPa; Figure 4). The large intraspecific variation in *C. mixtus* observed reflects earlier observations about the fuzzy boundaries between woodiness and herbaceousness (Lens, Eeckhout, Zwartjes, Smets, & Janssens, 2012; Lens, Smets et al., 2012). Indeed, nearly all the herbaceous species in angiosperms that do not belong to the monocots produce wood cells to some extent, but in small quantities and mainly confined to the base of the stem (Dulin & Kirchoff, 2010; Lens, Smets et al., 2012; Schweingruber, Borner, & Schulze, 2011). This continuous variation in wood formation often leads to intermediate life forms, referred in the literature as "woody herbs" or "half shrubs." As wood formation in the stems of these intermediate species (including *C. mixtus*) does not extend into the upper parts of the stem, we consider them not woody enough and thus herbaceous (Kidner et al., 2016).

4.4 | Relationship between embolism resistance vs. vessel grouping index, vessel density and ray abundance

Our general dataset shows that more embolism-resistant species have more vessels per xylem surface area (higher density of vessels—DE_V) compared to more vulnerable species. In addition, the general dataset and the woody dataset show that these vessels are grouped in larger multiples (higher vessel grouping index—G_V; Tables S2 and S3). Higher vessel grouping patterns allow the continuity of 3D water transport pathway in case one or several vessels in a vessel multiple become embolized (Carlquist, 1984; Lens et al., 2011). On the other hand, increased vessel–vessel contact areas facilitate the potential spread of air bubbles from one embolized vessel towards an adjacent functional one via air-seeding (Zimmermann, 1983). Therefore, the competitive advantage of having higher vessel grouping index may only be valid when the thickness of intervessel pit membrane is large enough to prevent air-seeding within the vessel multiple, which is statistically supported by a tight correlation between the thickness of intervessel pit membrane and vessel grouping index in the general and woody datasets, while the same correlation is not found for the herbaceous dataset with their thinner intervessel pit membranes.

Amongst the insular woody *Argyranthemum* species, there is a weakly significant, positive correlation between the proportion of ray area per wood area (P_R, as seen in tangential sections) and embolism resistance ($p = .04997$; $r = -.8784$; Table S2; Figure S3). We observed in the field that all the leaves of the embolism-resistant *Argyranthemum* species native to the drier regions were functionally dead at the end of the dry summer, while new green leaves were starting to flush after the first rains set in September 2013 (Figure S3b). In contrast, the most vulnerable (evergreen) *A. broussonetii*, always facing wet conditions throughout the year in its laurel forest habitat, shows less proportion of ray area per wood area (Figure S3c), although it is a much taller shrub (Figure S3a). It is known that ray tissue stores and transports water and carbohydrates via symplastic connections between inner bark and xylem through the vascular cambium (Pfautsch, Holtta, & Mencuccini, 2015; Pfautsch, Renard, Tjoelker, & Salih, 2015). Although speculative at this point, the higher proportion of rays in the more resistant species could be interpreted as a water/carbohydrate source that could reactivate meristematic cells at the end of the dormant summer period (Brodersen, McElrone, Choat, Matthews, & Shackel, 2010; Nardini, Lo Gullo, & Salleo, 2011; Spicer, 2014).

5 | CONCLUSIONS

We find that stems of the insular woody species of *Argyranthemum* are more resistant to drought-induced hydraulic failure than those of their herbaceous relatives native to the European mainland. Although this experimental result agrees with a marked drought signal in the ongoing global derived woodiness dataset including over 6000 derived woody flowering plant species representing several hundreds of transitions towards derived woodiness (F. Lens, unpublished data), this does not necessarily mean that drought has triggered wood formation in the common ancestor of *Argyranthemum* after arrival on the Canary Islands. Dated molecular phylogenies estimating the palaeoclimate in which the woody daisies have originated combined with a thorough niche modelling study including additional environmental variables (temperature, precipitation, aridity, potential evapotranspiration and soil) are likely to shed more light into this fascinating island phenomenon.

We show that intervessel pit membrane thickness best predicts the variation in embolism resistance amongst the daisy species studied and functionally explains P_{50} via its role in air-seeding. Moreover, the thickness of intervessel pit membrane is the essential missing link to understand the indirect correlation between embolism resistance and increased lignification, a correlation that has also been demonstrated in larger datasets (Hacke, Sperry et al., 2001; Lens et al., 2016; Pereira et al., 2017) as well as within species (Lens, Tixier et al., 2013; this study). Therefore, we argue that lignification characters do not have a direct impact on embolism resistance, but they co-evolve with other anatomical features that are more directly influencing P_{50} in water-conducting cells (Lachenbruch & McCulloh, 2014; Rosner, 2017).

ACKNOWLEDGEMENTS

L.C.D. appreciates the Graduate Research Fellowship from CNPq—Conselho Nacional de Desenvolvimento Científico e Tecnológico, Brazil, PROC. No. 206433/2014-0, and the Alberta Mennega Stichting for funding the collection trips and the visits to the Delzon lab. We also thank the Cabildo de Tenerife (AFF 147/13 No. Sigma: 2013-00748; AFF 429/13 No. Sigma: 2013-02030; AFF 149/15 No. Sigma: 2015-00925; AFF 85/16 No. Sigma: 2016-00838) and Teide National Park (No. 152587, REUS 27257, 2013; No. 536556, REUS 83804, 2013; Res. No. 222/2015) for the collection permits, and the Cluster of Excellence COTE (ANR-10-LABX-45) and the programme "Investments for the Future" (ANR-10-EQPX-16, XYLOFOREST) funded by the French National Agency for Research. We also acknowledge the technical support of R. Langelaan, W. Star and G. Capdeville.

CONFLICT OF INTEREST

The authors declare no conflict of interests.

AUTHORS' CONTRIBUTION

F.L. and S.D. conceived the ideas and designed methodology; L.C.D., M.A., T.C. and F.L. collected the data; L.C.D., D.S.P., S.D. and F.L. analysed the data; L.C.D. and F.L. wrote the manuscript, and all authors contributed critically with comments to the draft.

DATA ACCESSIBILITY

Data available from the Dryad Digital Repository https://doi.org/10.5061/dryad.sh546k0 (Dória et al., 2018).

ORCID

Larissa C. Dória http://orcid.org/0000-0002-3479-211X

Frederic Lens http://orcid.org/0000-0002-5001-0149

REFERENCES

Adams, H. D., Zeppel, M. J. B., Anderegg, W. R. L., Hartmann, H., Landhausser, S. M., Tissue, D. T., … Anderegg, L. D. (2017). A multi-species synthesis of physiological mechanisms in drought-induced tree mortality. *Nature Ecology & Evolution*, *1*, 1285–1291. https://doi.org/10.1038/s41559-017-0248-x

Anderegg, W. R. L., Klein, T., Bartlett, M., Sack, L., Pellegrini, A. F. A., Choat, B., & Jansen, S. (2016). Meta-analysis reveals that hydraulic traits explain cross-species patterns of drought-induced tree mortality across the globe. *Proceedings of the National Academy of Sciences of the United States of America*, *113*, 5024–5029. https://doi.org/10.1073/pnas.1525678113

Arechavaleta, M., Rodriguez, S., Zurita, N., & García, A. (2010). *Lista de especies silvestres de Canarias: hongos*, *plantas y animales terrestres* (p. 579). Tenerife, Spain: Gobierno de Canarias.

Awad, H., Herbette, S., Brunel, N., Tixier, A., Pilate, G., Cochard, H., & Badel, E. (2012). No trade-off between hydraulic and mechanical properties in several transgenic poplars modified for lignin metabolism. *Environmental and Experimental Botany*, *77*, 185–195. https://doi.org/10.1016/j.envexpbot.2011.11.023

Barigah, T. S., Charrier, O., Douris, M., Bonhomme, M., Herbette, S., Améglio, T., … Cochard, H. (2013). Water stress-induced xylem hydraulic failure is a causal factor of tree mortality in beech and poplar. *Annals of Botany*, *112*, 1431–1437. https://doi.org/10.1093/aob/mct204

Böhle, U. R., Hilger, H. H., & Martin, W. F. (1996). Island colonization and evolution of the insular woody habit in *Echium* L. (Boraginaceae). *Proceedings of the National Academy of Sciences of the United States of America*, *93*, 11740–11745. https://doi.org/10.1073/pnas.93.21.11740

Bouche, P. F., Larter, M., Domec, J. C., Burlett, R., Gasson, P., Jansen, S., & Delzon, S. (2014). A broad survey of xylem hydraulic safety and efficiency in conifers. *Journal of Experimental Botany*, *65*, 4419–4431. https://doi.org/10.1093/jxb/eru218

Brodersen, C. R., McElrone, A. J., Choat, B., Matthews, M. A., & Shackel, K. A. (2010). The dynamics of embolism repair in xylem: In vivo visualizations using high-resolution computed tomography. *Plant Physiology*, *154*, 1088–1095. https://doi.org/10.1104/pp.110.162396

Brodribb, T. J., Bowman, D., Nichols, S., Delzon, S., & Burlett, R. (2010). Xylem function and growth rate interact to determine recovery rates after exposure to extreme water deficit. *New Phytologist*, *188*, 533–542. https://doi.org/10.1111/j.1469-8137.2010.03393.x

Carlquist, S. (1974). Insular woodiness. In S. J. Carlquist (Ed.), *Island biology* (pp. 350–428). New York, NY: Columbia University Press.

Carlquist, S. (1984). Vessel grouping in dicotyledon wood: Significance and relationship to imperforate tracheary elements. *Aliso*, *10*, 505–525. https://doi.org/10.5642/aliso

Chevan, A., & Sutherland, M. (1991). Hierarchical partitioning. *The American Statistician*, *45*, 90–96.

Choat, B., Jansen, S., Brodribb, T. J., Cochard, H., Delzon, S., Bhaskar, R., … Jacobsen, A. L. (2012). Global convergence in the vulnerability of forests to drought. *Nature*, *491*, 752–756.

Cochard, H. (2002). A technique for measuring xylem hydraulic conductance under high negative pressures. *Plant, Cell and Environment*, *25*, 815–819. https://doi.org/10.1046/j.1365-3040.2002.00863.x

Cochard, H., Badel, E., Herbette, S., Delzon, S., Choat, B., & Jansen, S. (2013). Methods for measuring plant vulnerability to cavitation: A critical review. *Journal of Experimental Botany*, *64*, 4779–4791. https://doi.org/10.1093/jxb/ert193

Cochard, H., Barigah, T., Kleinhentz, M., & Eshel, A. (2008). Is xylem cavitation resistance a relevant criterion for screening drought resistance among *Prunus* species? *Journal of Plant Physiology*, *165*, 976–982. https://doi.org/10.1016/j.jplph.2007.07.020

Committee, I. A. W. A. (1989). IAWA list of microscopic features for hardwood identification. *IAWA Bulletin NS*, *10*, 219–332.

Darwin, C. (1859). *On the origin of species by means of natural selection* (reprint of 1st ed. 1950). London, UK: J. Murray.

Del-Arco, M., Pérez-de-Paz, P. L., Acebes, J. R., González-Mancebo, J. M., Reyes-Betancort, J. A., Bermejo, J. A., … González-González, R. (2006). Bioclimatology and climatophilous vegetation of Tenerife (Canary Islands). *Annales Botanici Fennici*, *43*, 167–192.

Dória, L. C., Podadera, D. S., del Arco, M., Chauvin, T., Smets, E., Delzon, S., & Lens, F. (2018). Data from: Insular woody daisies (*Argyranthemum*, Asteraceae) are more resistant to drought-induced hydraulic failure than their herbaceous relatives. *Dryad Digital Repository*, https://doi.org/10.5061/dryad.sh546k0

Doyle, J. A. (2012). Molecular and fossil evidence on the origin of angiosperms. *Annual Review of Earth and Planetary Sciences*, *40*, 301–326. https://doi.org/10.1146/annurev-earth-042711-105313

Dulin, M. W., & Kirchoff, B. K. (2010). Paedomorphosis, secondary woodiness and insular woodiness in plants. *Botanical review*, *76*, 405–490. https://doi.org/10.1007/s12229-010-9057-5

Francisco-Ortega, J., Crawford, D. J., Santos-Guerra, A., & Jansen, R. K. (1997). Origin and evolution of *Argyranthemum* (Asteraceae: Anthemideae) in Macaronesia. In T. J. Givnish & K. J. Sytsma (Eds.), *Molecular evolution and adaptive radiation* (pp. 407–431). Cambridge, UK: Cambridge University Press.

Givnish, T. J. (1998). Adaptive plant evolution on islands: Classical patterns, molecular data, new insights. In P. R. Grant (Ed.), *Evolution on Islands* (pp. 281–304). Oxford, UK: Oxford University Press.

Gleason, S. M., Westoby, M., Jansen, S., Choat, B., Brodribb, T. J., Cochard, H., … Lens, F. (2016). On research priorities to advance understanding of the safety-efficiency trade off in xylem. *New Phytologist*, *211*, 1156–1158. https://doi.org/10.1111/nph.14043

Hacke, U. G., Sperry, J. S., Pockman, W. T., Davis, S. D., & McCulloh, K. A. (2001). Trends in wood density and structure are linked to prevention of xylem implosion by negative pressure. *Oecologia*, *126*, 457–461. https://doi.org/10.1007/s004420100628

Hacke, U. G., Stiller, V., Sperry, J. S., Pittermann, J., & McCulloh, K. A. (2001). Cavitation fatigue. Embolism and refilling cycles can weaken the cavitation resistance of xylem. *Plant Physiology*, *125*, 779–786. https://doi.org/10.1104/pp.125.2.779

Hamann, T. D., Smets, E., & Lens, F. (2011). A comparison of paraffin and resin-based techniques used in bark anatomy. *Taxon*, *60*, 841–851.

Hoffman, W. A., Marchin, R. M., Abit, P., & Lau, L. O. (2011). Hydraulic failure and tree dieback are associated with high wood density in a temperate forest under extreme drought. *Global Change Biology*, *17*, 2731–2742. https://doi.org/10.1111/j.1365-2486.2011.02401.x

Humphries, C. J. (1976). A revision of the Macaronesian genus *Argyranthemum* Webb ex Schultz-Bip. (Compositae-Anthemideae). *Bulletin of the British Museum (Natural History) Botany*, *5*, 147–240.

Jacobsen, A. L., Ewers, F. W., Pratt, R. B., Paddock, W. A., & Davis, D. (2005). Do xylem fibers affect vessel cavitation resistance? *Plant Physiology*, *139*, 546–556. https://doi.org/10.1104/pp.104.058404

Jansen, S., Choat, B., & Pletsers, A. (2009). Morphological variation of intervessel pit membranes and implications to xylem function in angiosperms. *American Journal of Botany*, *96*, 409–419. https://doi.org/10.3732/ajb.0800248

Karnovsky, M. J. (1965). A formaldehyde - glutaraldehyde fixative of high osmolality for use in electron microscopy. *Journal of Cell Biology*, *27*, 137–138.

Kidner, C., Groover, A., Thomas, D., Emelianova, K., Soliz-Gamboa, C., & Lens, F. (2016). First steps in studying the origins of secondary woodiness in *Begonia* (Begoniaceae): Combining anatomy, phylogenetics, and stem transcriptomics. *Biological Journal of the Linnean Society*, *117*, 121–138. https://doi.org/10.1111/bij.12492

Lachenbruch, B., & McCulloh, K. A. (2014). Traits, properties, and performance: How woody plants combine hydraulic and mechanical functions in a cell, tissue, or whole plant. *New Phytologist*, *204*, 747–764. https://doi.org/10.1111/nph.13035

Larter, M., Brodribb, T. J., Pfautsch, S., Burlett, R., Cochard, H., & Delzon, S. (2015). Extreme aridity pushes trees to their physical limits. *Plant Physiology*, *168*, 804–807. https://doi.org/10.1104/pp.15.00223

Lefcheck, J. S. (2015). piecewiseSEM: Piecewise structural equation modelling in R for ecology, evolution, and systematics. *Methods in Ecology and Evolution*, *7*, 573–579.

Lens, F., Davin, N., Smets, E., & del Arco, M. (2013). Insular woodiness on the Canary Islands: Remarkable case of convergent evolution. *International Journal of Plant Sciences*, *174*, 992–1013. https://doi.org/10.1086/670259

Lens, F., Eeckhout, S., Zwartjes, R., Smets, E., & Janssens, S. (2012). The multiple fuzzy origins of woodiness within Balsaminaceae using an integrated approach. Where do we draw the line? *Annals of Botany*, *109*, 783–799. https://doi.org/10.1093/aob/mcr310

Lens, F., Picon-Cochard, C., Delmas, C., Signarbieux, C., Buttler, A., Cochard, H., … Delzon, S. (2016). Herbaceous angiosperms are not more vulnerable to drought-induced embolism than angiosperm trees. *Plant Physiology*, *172*, 661–667.

Lens, F., Smets, E., & Melzer, S. (2012). Stem anatomy supports *Arabidopsis thaliana* as a model for insular woodiness. *New Phytologist*, *193*, 12–17. https://doi.org/10.1111/j.1469-8137.2011.03888.x

Lens, F., Sperry, J. S., Christman, M. A., Choat, B., Rabaey, D., & Jansen, S. (2011). Testing hypotheses that link wood anatomy to cavitation resistance and hydraulic conductivity in the genus *Acer*. *New Phytologist*, *190*, 709–723. https://doi.org/10.1111/j.1469-8137.2010.03518.x

Lens, F., Tixier, A., Cochard, H., Sperry, J. S., Jansen, S., & Herbette, S. (2013). Embolism resistance as a key mechanism to understand adaptive plant strategies. *Current Opinion in Plant Biology*, *16*, 287–292. https://doi.org/10.1016/j.pbi.2013.02.005

Li, S., Lens, F., Espino, S., Karimi, Z., Klepsch, M., Schenk, H. J., … Jansen, S. (2016). Intervessel pit membrane thickness as a key determinant of embolism resistance in angiosperm xylem. *IAWA Journal*, *37*, 152–171. https://doi.org/10.1163/22941932-20160128

Maherali, H., Pockman, W. T., & Jackson, R. (2004). Adaptive variation in the vulnerability of woody plants to xylem cavitation. *Ecology*, *85*, 2184–2199. https://doi.org/10.1890/02-0538

Nakagawa, S., & Schielzeth, H. (2013). A general and simple method for obtaining R^2 from generalized linear mixed-effect models. *Methods in Ecology and Evolution*, *4*, 133–142. https://doi.org/10.1111/j.2041-210x.2012.00261.x

Nardini, A., Lo Gullo, M. A., & Salleo, S. (2011). Refilling embolized xylem conduits: Is it a matter of phloem unloading? *Plant Science*, *180*, 604–611. https://doi.org/10.1016/j.plantsci.2010.12.011

Oberprieler, C., Himmelreich, S., Källersjö, M., Vallès, J., Watson, L. E., & Vogt, R. (2009). Anthemideae. In V. A. Funk, A. Susanna, T. F. Stuessy, & R. J. Bayer (Eds.), *Systematics, evolution, and biogeography of Compositae* (pp. 631–666). Vienna, Austria: International Association for Plant Taxonomy.

Pammenter, N. W., & Van der Willigen, C. (1998). A mathematical and statistical analysis of the curves illustrating vulnerability of xylem to cavitation. *Tree Physiology*, *18*, 589–593. https://doi.org/10.1093/treephys/18.8-9.589

Pereira, L., Domingues-Junior, A. P., Jansen, S., Choat, B., & Mazzafera, P. (2017). Is embolism resistance in plant xylem associated with quantity and characteristics of lignin? *Trees*, *31*. https://doi.org/10.1007/s00468-017-1574-y

Pfautsch, S., Holtta, T., & Mencuccini, M. (2015). Hydraulic functioning of tree stems: Fusing ray anatomy, radial transfer and capacitance. *Tree Physiology*, *35*, 706–722. https://doi.org/10.1093/treephys/tpv058

Pfautsch, S., Renard, J., Tjoelker, M. G., & Salih, A. (2015). Phloem as capacitor: Radial transfer of water into xylem of tree stems occurs via symplastic transport in ray parenchyma. *Plant Physiology*, *167*, 963–971. https://doi.org/10.1104/pp.114.254581

Pinheiro, J., Bates, D., DebRoy, S., Sarkar, D., & R Core Team (2016). *nlme: linear and nonlinear mixed effects models*. R package version 3.1-126. Retrieved from http://CRAN.R-project.org/package=nlme

R Core Team (2016). *R: A language and environment for statistical computing*. Vienna, Austria: R Foundation for Statistical Computing. Retrieved from https://www.r-project.org/

Rosner, S. (2017). Wood density as a proxy for vulnerability to cavitation: Size matters. *The Journal of Plant Hydraulics*, *4*, 1–10. https://doi.org/10.20870/jph.2017.e001

Schenk, J. H., Espino, S., Romo, D. M., Nima, N., Do, A. Y. T., Michaud, J. M., … Jansen, S. (2017). Xylem surfactants introduce a new element to the cohesion-tension theory. *Plant Physiology*, *173*, 1177–1196. https://doi.org/10.1104/pp.16.01039

Schenk, H. J., Steppe, K., & Jansen, S. (2015). Nanobubbles: A new paradigm for air-seeding in xylem. *Trends in Plant Science*, *20*, 199–205. https://doi.org/10.1016/j.tplants.2015.01.008

Scholz, A., Klepsch, M., Karimi, Z., & Jansen, S. (2013). How to quantify conduits in wood? *Frontiers in Plant Science*, *56*, 1–11.

Schweingruber, F. H., Borner, A., & Schulze, E. D. (2011). *Atlas of stem anatomy in herbs, shrubs and trees*, Vol. *1*. Heidelberg, Germany: Springer. https://doi.org/10.1007/978-3-642-11638-4

Sperry, J. S. (2003). Evolution of water transport and xylem structure. *International Journal of Plant Science*, *164*, 115–127. https://doi.org/10.1086/368398

Sperry, J. S., Nichols, K. L., & Sullivan, J. E. M. (1994). Xylem embolism in ring-porous, diffuse-porous, and coniferous trees of Northern Utah and Interior Alaska. *Ecology*, *75*, 1736–1752. https://doi.org/10.2307/1939633

Spicer, R. (2014). Symplasmic networks in secondary vascular tissues: Parenchyma distribution and activity supporting long-distance transport. *Journal of Experimental Botany*, *65*, 1829–1848. https://doi.org/10.1093/jxb/ert459

Trueba, S., Pouteau, R., Lens, F., Feild, T. S., Isnard, S., Olson, M. E., & Delzon, S. (2017). Vulnerability to xylem embolism as a major correlate of the environmental distribution of rainforest species on a tropical island. *Plant, Cell and Environment*, *40*, 277–289. https://doi.org/10.1111/pce.12859

Tyree, M. T., & Zimmermann, M. H. (2002). *Xylem structure and the ascent of sap* (2nd ed.). Berlin, Germany: Springer-Verlag Press. https://doi.org/10.1007/978-3-662-04931-0

Urli, M., Porté, A. J., Cochard, H., Guengant, Y., Burlett, R., & Delzon, S. (2013). Xylem embolism threshold for catastrophic hydraulic failure in angiosperm trees. *Tree Physiology*, *33*, 672–683. https://doi.org/10.1093/treephys/tpt030

Wallace, A. R. (1878). *Tropical nature and other essays*. London, UK: Macmillan Press. https://doi.org/10.5962/bhl.title.1261

Zieminska, K., Butler, D. W., Gleason, S. M., Wright, I. J., & Westoby, M. (2013). Fibre wall and lumen fractions drive wood density variation across 24 Australian angiosperms. *Annals of Botany*, *5*, 1–14.

Zieminska, K., Westoby, M., & Wright, I. J. (2015). Broad anatomical variation within a narrow wood density range – A study of twig wood across 69 Australian angiosperms. *PLoS ONE*, *10*, 1–25.

Zimmermann, M. H. (1983). *Xylem structure and the ascent of sap*. Berlin, Germany: Springer-Verlag Press. https://doi.org/10.1007/978-3-662-22627-8

Zuur, A. F., Ieno, E. N., & Elphick, C. S. (2010). A protocol for data exploration to avoid common statistical problems. *Methods in ecology and evolution*, *1*, 3–14. https://doi.org/10.1111/j.2041-210X.2009.00001.x

Zuur, A. F., Ieno, E. N., Walker, N., Saveliev, A. A., & Smith, G. M. (2009). *Mixed effects models and extensions in ecology with R*. New York, NY: Springer. https://doi.org/10.1007/978-0-387-87458-6

SUPPORTING INFORMATION

Additional Supporting Information may be found online in the supporting information tab for this article.

How to cite this article: Dória LC, Podadera DS, del Arco M, et al. Insular woody daisies (*Argyranthemum*, Asteraceae) are more resistant to drought-induced hydraulic failure than their herbaceous relatives. *Funct Ecol*. 2018;32:1467–1478. https://doi.org/10.1111/1365-2435.13085